

# Facile Synthesis and Highly Reactive Silver Ion Adsorption of Novel Microparticles of Sulfodiphenylamine and Diaminonaphthalene Copolymers

Xin-Gui Li,<sup>\*,†,‡</sup> Rui Liu,<sup>†</sup> and Mei-Rong Huang<sup>\*,†</sup>

*Institute of Materials Chemistry, School of Materials Science and Engineering, Tongji University, 1239 Siping Road, Shanghai 200092, China, and Department of Chemistry and Chemical Biology, Harvard University, 12 Oxford Street, Cambridge, Massachusetts 02138*

Received April 18, 2005. Revised Manuscript Received August 25, 2005

A series of novel copolymer microparticles from 4-sulfonic diphenylamine (SDP) and 1,8-diaminonaphthalene (DAN) was readily prepared by a chemically oxidative polymerization. The structures and properties of the microparticles were systematically characterized by several important techniques. The microparticles exhibit good water resistance and high thermostability. Their electrical conductivity significantly rises after HCl doping or Ag adsorption. The Ag<sup>+</sup> reactive adsorbability of the microparticles was optimized by carefully regulating the SDP/DAN ratio, particle size, and Ag<sup>+</sup> solution pH. Both the introduction of SDP units into DAN polymer chains and the diminution of the particle size can effectively increase the capacity and rate of Ag<sup>+</sup> adsorption. In particular, the Ag<sup>+</sup> adsorbance on SDP/DAN (30/70) copolymer microparticles reaches 2.0 g g<sup>-1</sup>, which is the highest silver adsorption capacity reported thus far. A novel mechanism of Ag<sup>+</sup> reactive adsorption on the microparticles containing a large number of reactive groups such as amino, imino, and sulfonic groups has been proposed. The microparticles could be very applicable to elimination and recovery of noble metallic ions in wastewater.

## Introduction

Aromatic amine polymers have exhibited wide technological applications, such as rechargeable batteries,<sup>1</sup> electrocatalysts,<sup>2</sup> smart windows, microelectronic and electrochromic devices,<sup>3</sup> sensors,<sup>4</sup> and actuators,<sup>5</sup> due to their novel multifunctionality, including good redox reversibility,<sup>6</sup> variable conductivity,<sup>6,7</sup> strong electroactivity,<sup>2</sup> colorful electrochromism,<sup>3</sup> and high environmental stability. Heavy metals in wastewater have long been a concern due to environmental and health problems. Adsorption is considered an effective method for removing these heavy metals. Some adsorbents, such as metal oxide,<sup>8</sup> activated carbon,<sup>9</sup> and biomaterial,<sup>10</sup> have traditionally been employed to remove heavy metals from solution. Recently, poly(1,8-diaminonaphthalene) (PDAN) has attracted more attention of researchers in

extraction and adsorption of heavy metal ions, due to its highly reactive sensitivity to the metal ions, including Ag<sup>+</sup>, Cu<sup>2+</sup>, Hg<sup>2+</sup>, Pb<sup>2+</sup>, VO<sup>2+</sup>, and Cr<sup>3+</sup>, via complexation or reduction with the amino/imino groups on the PDAN.<sup>11,12</sup> However, most studies are concentrated on electrosynthesized PDAN film with small specific area and low preparation yield, which largely restricts its efficient and inexpensive application for the removal or recovery of the heavy metals from solutions. As an alternative way, chemically oxidative polymerization has been successfully employed to synthesize aniline (AN) and pyrrole copolymers.<sup>13–16</sup> Unfortunately, the method has hardly ever been used for the synthesis of the PDAN microparticles. Meanwhile, it has been demonstrated that the adsorbent particles of smaller size usually exhibit higher adsorbability of heavy metal ions, because of much larger specific area. For example, carbon nanobeads can very quickly extract Au<sup>3+</sup>, Ag<sup>+</sup>, Pd<sup>+</sup>, and Pt<sup>+</sup> from their aqueous solution,<sup>17</sup> achieving 95% removal in less than 10 min. The introduction of sulfonic groups into polyaniline (PAN) chains has proved to be the simplest and most effective method of obtaining fine AN copolymer particles.<sup>18,19</sup>

\* To whom correspondence should be addressed. E-mail: adamxgli@yahoo.com (X.G.L.), huangmeirong@tongji.edu.cn (M.R.H.).

<sup>†</sup> Tongji University.

<sup>‡</sup> Harvard University.

- (1) Torres-Gomez, G.; Tejada-Rosales, E. M.; Gomez-Romero, P. *Chem. Mater.* **2001**, *13*, 3693.
- (2) Li, X. G.; Huang, M. R.; Duan, W.; Yang, Y. L. *Chem. Rev.* **2002**, *102*, 2925.
- (3) Boehme, J. L.; MudigoDAN, D. S. K.; Ferraris, J. P. *Chem. Mater.* **2001**, *13*, 4469.
- (4) Virji, S.; Kaner, R. B.; Weiller, B. H. *Chem. Mater.* **2005**, *17*, 1256.
- (5) Lu, W.; Smela, E.; Adams, P.; Zuccarello, G.; Mattes, B. R. *Chem. Mater.* **2004**, *16*, 1615.
- (6) Yue, J.; Wang, Z. H.; Cromack, K. R.; Epstein, A. J.; MacDiarmid, A. J. *J. Am. Chem. Soc.* **1991**, *113*, 2665.
- (7) Wei, X. L.; Wang, Y. Z.; Long, S. M.; Bobeczko, C.; Epstein, A. J. *J. Am. Chem. Soc.* **1996**, *118*, 2545.
- (8) Crawford, R. J.; Mainwaring, D. E.; Harding, I. H. *Colloids Surf. A* **1997**, *126*, 167.
- (9) Yue, Z. R.; Jiang, W.; Wang, L.; Toghiani, H.; Gardner, S. D.; Pittman, C. U., Jr. *Carbon* **1999**, *37*, 1607.
- (10) Sag, Y.; Atacoglu, I.; Kutsal, T. *Hydrometallurgy* **2000**, *55*, 165.

- (11) Lee, J. W.; Park, D. S.; Shim, Y. B.; Park, S. M. *J. Electrochem. Soc.* **1992**, *139*, 3507.
- (12) Palys, B. J.; Skompska, M.; Jackowska, K. *J. Electroanal. Chem.* **1997**, *433*, 41.
- (13) Li, X. G.; Duan, W.; Huang, M. R.; Yang, Y. L.; Zhao, D. Y.; Dong, Q. *Z. Polymer* **2003**, *44*, 5579.
- (14) Li, X. G.; Huang, M. R.; Hua, Y. M. *Macromolecules* **2005**, *38*, 4211.
- (15) Li, X. G.; Chen, R. F.; Huang, M. R.; Zhu, M. F.; Chen, Q. *J. Polym. Sci., Part A, Polym. Chem.* **2004**, *42*, 2073.
- (16) Li, X. G.; Huang, M. R.; Lu, Y. Q.; Zhu, M. F. *J. Mater. Chem.* **2005**, *15*, 1343.
- (17) An, X. N.; Zeng, H. M. *Carbon* **2003**, *41*, 2889.

Therefore, we employed the chemically oxidative polymerization of 1,8-diaminonaphthalene (DAN) and 4-sulfonic diphenylamine (SDP) to directly synthesize fine SDP/DAN copolymer microparticles as a novel sorbent for effective extraction of  $\text{Ag}^+$  ion. The macromolecular and supramolecular structures, physicochemical properties, and especially the  $\text{Ag}^+$  adsorption of the copolymer microparticles were studied. The effect of the SDP/DAN comonomer ratio, particle size, concentration and pH of  $\text{Ag}^+$  solution, and adsorption time on the  $\text{Ag}^+$  reactive adsorbability of the microparticles was elaborated and optimized for the first time.

## Experimental Section

**Chemical Oxidative Polymerization.** 1,8-Diaminonaphthalene (DAN), sodium diphenylamine-4-sulfonate, ammonium persulfate, acetonitrile, and silver nitrate of analytical reagent grade were commercially obtained and used as received. A typical preparation procedure of the SDP/DAN (10/90) copolymer microparticles by the chemically oxidative precipitation polymerization in neutral acetonitrile/water solution is as follows: to 25 mL of acetonitrile at 20 °C was added 0.711 g (4.5 mmol) of DAN and to 25 mL of water was added 0.136 g (0.5 mmol) of SDP. The monomer solutions were mixed in a 200-mL glass flask. Ammonium persulfate (1.14 g, 5 mmol) was dissolved separately in 50 mL of distilled water to prepare an oxidant solution. The oxidant solution was then dropped into the mixed monomer solution at a rate of one drop (60  $\mu\text{L}$ ) every 3 s at 20 °C with a final comonomer/oxidant molar ratio of 1/1. The reaction mixture was vigorously magnetically stirred for 6 h at 20 °C. The open-circuit potential and temperature of the polymerization solution were recorded continuously. The resulting polymer precipitates were filtered and washed thoroughly with water to remove the residual oxidant, water-soluble oligomers, and byproducts. The solid microparticles were left to dry in ambient air at 40 °C for 3 days. The polymer microparticles of 0.69 g were obtained with the yield of ca. 82%.

**Measurements.** The open-circuit potential was measured with a potentiometer with a saturated calomel electrode as reference electrode and platinum foil as the counter electrode. The IR spectra were recorded on Nicolet Magna 550 FT-IR spectrometer at 2  $\text{cm}^{-1}$  resolution on KBr pellets. UV-vis spectra of the polymers in NMP were obtained on Perkin-Elmer Instruments Lambda 35 at a scanning rate of 480  $\text{nm min}^{-1}$ . The elemental analysis was carried out on a Carlo Erba 1106 element analyzer. Solid-state  $^{13}\text{C}$  NMR spectra were taken on Bruker DSX 300 at 75.39 MHz. The insolubility of the particles was evaluated using the following method: Polymer powders (5 mg) were added into the solvent (1 mL) and dispersed thoroughly. After the mixture was swayed continuously for 24 h at room temperature, the insolubility was characterized. The bulk electrical conductivity of the polymers was measured by a two-disk method using a UT 70A multimeter at ambient temperature. Thermogravimetric measurements were performed at a heating rate of 10 °C  $\text{min}^{-1}$  with the sample size of 1.3–1.6 mg using a NETZSCH-GERATEBAU GmbH thermal analyzer in static air. Wide-angle X-ray diffraction was performed with a D8 Advance X with Cu K $\alpha$  radiation at a scanning rate of 0.888°  $\text{min}^{-1}$ . The size of the polymer particles in water was analyzed with an LS230 laser particle-size analyzer from Beckman Coulter, Inc. Nitrogen adsorption-desorption isotherms were measured with

a Micromeritics Tristar 3000 analyzer at 77 K. The Barrett–Emmett–Teller (BET) method was utilized to calculate the surface area. The pore volume and pore-size distributions were derived from the adsorption branches of the isotherms using the Barrett–Joyner–Haladan (BJH) method.

**Reactive Adsorption of  $\text{Ag}^+$ .** The adsorption of  $\text{Ag}^+$  in aqueous solution on SDP/DAN polymer particles as an adsorbent was performed in a batch experiment.  $\text{Ag}^+$  aqueous solution (25 mL) at an  $\text{Ag}^+$  concentration range from 0.1 to 100 mM was incubated with a given amount of the particles at a fixed temperature of 30 °C. After a desired treatment period, the particles were filtered from the solution and then the concentration of  $\text{Ag}^+$  in the filtrate was measured by molar titration at higher  $\text{Ag}^+$  concentration or inductively coupled plasma at lower  $\text{Ag}^+$  concentration. The adsorbed amount of  $\text{Ag}^+$  on the microparticles was calculated according to eqs 1 and 2

$$Q = (C_0 - C)VM/W \quad (1)$$

$$q = [(C_0 - C)/C_0] \times 100\% \quad (2)$$

where  $Q$  is the adsorption capacity,  $q$  is the adsorptivity,  $C_0$  and  $C$  are  $\text{Ag}^+$  concentrations before and after adsorption, respectively,  $V$  is the initial volume of the  $\text{Ag}^+$  solution;  $M$  is the molecular weight of  $\text{Ag}^+$ , and  $W$  is the weight of the microparticles added.

**Mathematical Modeling.** The Lagergren expression of  $\text{Ag}^+$  adsorption rate on the microparticles is as follows

$$-\ln(1 - F) = kt \quad (3)$$

where  $F$  equals  $Q_t/Q_e$ ,  $Q_e$  is the amount adsorbed at equilibrium,  $Q_t$  is the amount adsorbed at time  $t$ , and  $k$  is the adsorption rate constant.

Two linearized adsorption models of Langmuir and Freundlich isotherms were used to analyze adsorption equilibrium in eqs 4 and 5, respectively:

$$C_e/Q_e = C_e/Q_m + 1/(KQ_m) \quad (4)$$

$$\ln Q_e = \ln K_3 + (1/n) \ln C_e \quad (5)$$

where  $C_e$  is the  $\text{Ag}^+$  equilibrium concentration,  $Q_e$  is the adsorption capacity,  $Q_m$  and  $K$  are the Langmuir constants related to the saturated adsorption capacity and energy, respectively,  $K_3$  is the equilibrium constant indicative of adsorption capacity, and  $n$  is the adsorption equilibrium constant. These constants were evaluated from the intercept and slope, respectively, of the linear plots of  $C_e/Q_e$  vs  $C_e$ , and  $\ln Q_e$  vs  $\ln C_e$ .

## Results and Discussion

**Synthesis of the Fine Microparticles of the SDP/DAN Polymers.** The chemical oxidative polymerization of SDP and DAN comonomers in acetonitrile/water simply and directly affords fine, uniform, and black microparticles as products. Progress in the polymerization reaction was in situ, followed by testing the temperature and open-circuit potential of the polymerization solution. It is found that with slowly dropping oxidant solution, both the temperature and potential rise gradually at first, then pass through top values, and finally remain nearly constant. The SDP/DAN polymerization is exothermic and the enhancement ( $\Delta T$ ) of the solution temperature steadily decreases from 3.4 to 0.5 °C with increasing SDP feed content from 0 to 50 mol % (Table S1, Supporting Information). This is possibly due to the low polymerizing capability of SDP monomer compared with

(18) Li, X. G.; Huang, M. R.; Feng, W.; Zhu, M. F.; Chen, Y. M. *Polymer* **2004**, *45*, 101.

(19) Li, X. G.; Zhou, H. J.; Huang, M. R.; Zhu, M. F.; Chen, Y. M. *J. Polym. Sci., Part A, Polym. Chem.* **2004**, *42*, 3380.

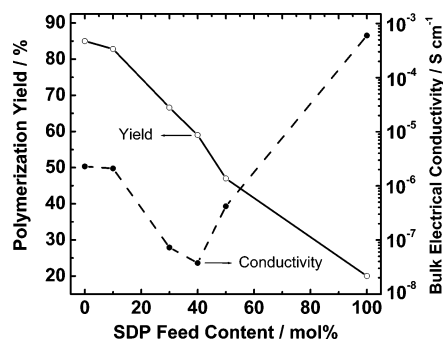


**Figure 1.** Polymerization yield and bulk electrical conductivity of SDP/DAN copolymer microparticles as a function of SDP feed content. The sample for the conductivity measurement is HCl-doped microparticles that were prepared by treating the as-polymerized microparticles in 1 M HCl for 24 h.

DAN monomer. The top potential shows a basically enhanced trend from 294 to 302 to 466 mV vs SCE at the polymerization time of around 30–33 min as SDP content increases from 0 to 10 to 50 mol %. The enhancement of the top potential with an increase in SDP content also suggests the low polymerizability of SDP monomer, which could be ascribed to (1) the higher oxidation potential of SDP monomer (0.86 V) than DAN monomer (0.44 V)<sup>20,21</sup> and (2) the electron withdrawing and great steric effects of the sulfophenylene side group. This behavior coincided with the copolymerization of ethylaniline with sulfoanisidine.<sup>18</sup> The final potential of the copolymerization solutions, as a signal of the redox state of as-formed polymer chains, changes from 250 to 236 to 410 mV vs SCE with increasing SDP content from 0 to 10 to 50 mol % under the same initial potential of 210 mV vs SCE. Note that the SDP/DAN (10/90) copolymerization solution exhibits the lowest final potential. This nonmonotonic variation of final potential with SDP/DAN ratio could signify that a real copolymerization between the SDP and DAN comonomers occurs. A similar phenomenon has been found for the ethylaniline/sulfoanisidine copolymerization in our laboratory.

As shown in Figure 1, the polymerization yield strongly depends on the SDP/DAN ratio. The yield decreases monotonically from 85 to 20% as the SDP content increases from 0 to 100 mol %.<sup>19</sup> The lower yield at higher SDP feed content is also attributable to the weaker polymerizability of the SDP monomer than the DAN monomer. A basically similar variation of the yield with SDP content was found for the copolymers of AN and *o*-aminobenzyl alcohol with SDP monomer, respectively.<sup>19,20</sup>

**Structure Analysis of Copolymer Microparticles.** The macromolecular structure of SDP/DAN (0/100 and 30/70) polymers has been conjectured from C/H/N/S ratio determined by element analysis, as listed in Table 1. Obviously, the PDAN structure derived from element ratio suggests that a denitrogenation happens during the polymerization. However, the structure of DAN units in the copolymer contains more  $\text{—NH—}$  units due to lower denitrogenation than PDAN. Slightly higher experimental H content in the copolymer must result from hydrophilicity of the copolymer owing to the

presence of the  $\text{—SO}_3\text{H}$  group. It is further seen that the SDP unit content in the copolymer is significantly lower than the SDP feed content, due to the lower polymerizability of SDP monomer than DAN monomer, as discussed above.

FT-IR spectra (Figure S1, Supporting Information) of the SDP/DAN copolymers illustrate a broad and strong band centered at  $3385\text{ cm}^{-1}$  due to the characteristic stretching vibration of free N—H bond, suggesting the presence of a large amount of amino and imino groups ( $\text{—NH}_2$  and  $\text{—NH—}$ ) in the polymers. A small peak at  $2920\text{ cm}^{-1}$  from the C—H stretching vibration on naphthalene unit in the polymers shifts to a higher wavenumber with increasing SDP content. The IR absorptions at  $1730$  and  $1623\text{ cm}^{-1}$  are associated with quinoid and benzenoid ring stretching, respectively. It can be seen that the ratio of peak intensity for  $1730$  over  $1623\text{ cm}^{-1}$  increases first and then decreases with an increase in SDP content from 0 to 50 mol %. Actually, the SDP/DAN (30/70) copolymer among five polymers exhibits the highest ratio of peak intensity at  $1730$  over  $1623\text{ cm}^{-1}$ . Moreover, a similar variation of the peak intensities at  $1252$  and  $1050\text{ cm}^{-1}$  ascribed to asymmetric and symmetric stretchings of the S=O bond in the SDP unit, respectively, was observed with SDP/DAN ratio, i.e., the strongest bands also appear in the IR spectrum of the SDP/DAN (30/70) copolymer. This strongly suggests a complicated structure variation with SDP/DAN ratio. In other words, the SDP/DAN polymer obtained thus is a real copolymer between both comonomers rather than a simple mixture of both homopolymers. The out-of-plane C—H bending modes appeared in the PDAN spectrum at  $770$ ,  $696$ , and  $617\text{ cm}^{-1}$ , indicating the 1,4,8-trisubstituted naphthalene ring. The bands merge into a very broad band after the introduction of SDP unit into PDAN chain due to the appearance of absorption bands from the C—S, S=O, and 1,4-disubstituted benzenoid ring in SDP units.

The UV–vis spectra (Figure S2, Supporting Information) of the polymers exhibit two groups of bands: three coalescent bands centered at 265 (strong), 302 (medium), 355 (weak) nm due to  $\pi\text{—}\pi^*$  transition from the benzenoid ring and a very weak band centered at 500 nm due to  $n\text{—}\pi^*$  excitation or interband charge transfer associated with the excitation of benzenoid to quinoid rings. All of the bands steadily become weaker with increasing SDP content due to an increased insolubility of the polymers in NMP (Table S1, Supporting Information). The ratio of band intensity at 500 nm over 265–355 nm increases with increasing SDP content, signifying a higher concentration of quinone units in the copolymers with higher SDP content.

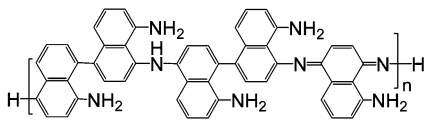
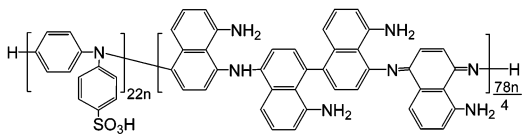
Because of limited solubility of SDP/DAN copolymers in DMSO and  $\text{CHCl}_3$ , solid-state  $^{13}\text{C}$  NMR is further utilized to characterize the macromolecular structure of the SDP/DAN (0/100 and 30/70) polymers. PDAN exhibits seven resonance peaks that are assigned to aromatic carbons at 114 ppm (strongest), 121 ppm (strong), 124 ppm (strong), 129 ppm (strong), 136 ppm (medium), 144 ppm (weak), and 189 ppm (very weak), while the SDP/DAN (30/70) copolymer exhibits six resonance peaks to aromatic carbons at 121 ppm (strongest), 129 ppm (strong), 135 ppm (strong), 143 ppm (medium), 151 ppm (weak), and 200–215 ppm (very weak). Apparently the copolymer exhibits higher chemical shift, i.e.,

(20) Nguyen, M. T.; Diaz, A. F. *Macromolecules* **1994**, *27*, 7003.

(21) Skompska, M.; Hillman, A. R. *J. Chem. Soc., Faraday Trans.* **1996**, *92*, 4101.



Table 1. Elemental Analysis and Possible Macromolecular Structures of SDP/DAN Polymer Microparticles

Polymer	PDAN	SDP/DAN (30/70) copolymer
C / H / N / S / Total (wt%)	72.77/4.18/13.37/ - /90.32	62.88/4.06/11.02/3.73/81.69
Experimental formula	$C_{10}H_{6.90}N_{1.58}$	$C_{10}H_{7.76}N_{1.49}S_{0.22}$
Calculated formula and proposed macromolecular structure	$C_{10}H_{7.20}N_{1.60}$ 	$C_{10}H_{7.32}N_{1.52}S_{0.21}$ 

higher aromaticity, that coincided with its higher insolubility in DMSO, DMF, and  $CHCl_3$  (Table S1, Supporting Information). Besides, the carbon peaks of the copolymer at 114–144 ppm are relatively symmetrical, whereas those of PDAN are quite asymmetrical. All of these imply that the molecular structure of the SDP/DAN (30/70) copolymer is substantially different from that of the PDAN.

The supramolecular structure of the polymer particles has been characterized by a wide-angle X-ray diffraction technique (Figure S3, Supporting Information). PDAN exhibits two diffraction peaks at Bragg angles of  $13.0^\circ$  (strong) and  $23.9^\circ$  (medium), while the two peaks become unobvious and merge into one broad peak with introducing a SDP unit into the PDAN chain. It is interesting that the strong peak at  $13.0^\circ$  dramatically becomes weaker and shifts to a larger angle upon introducing a SDP unit, whereas the medium peak at  $23.9^\circ$  becomes stronger but the diffraction angle substantially remains constant at  $23.9^\circ$ . These results indicate that the crystalline structure of the microparticles varies significantly with SDP/DAN ratio, i.e., SDP/DAN copolymer microparticles exhibit lower crystallinity than PDAN microparticles because a great steric effect of sulfophenylene side groups on the SDP units leads to irregular arrangement of the copolymer chains. Low crystalline or high amorphous structure should be advantageous to the achievement of high adsorption ability, because the metal ion can easily diffuse into relatively irregular and loose microparticles. This intricate variation of diffraction characteristics with SDP/DAN ratio also signifies that the obtained SDP/DAN polymers are real copolymers, as mentioned above.

The size of the polymer particles has been systematically characterized by laser particle-size analysis. As shown in Figure 2, with increasing SDP content from 0 to 50 mol %, the number-average diameter ( $D_n$ ) of the as-prepared particles (ultrasonic treatment time = 0 h) monotonically increases from 3.582 to  $10.124 \mu\text{m}$ , while the size polydispersity index ( $D_w/D_n$ ) exhibits a minimum (1.246) at the SDP content of 10 mol %. It is reported that the introduction of sulfonic side group into PAN chain may dramatically reduce the size of PAN particles due to the static repulsion of the negatively charged sulfonic groups.<sup>18,19</sup> However, there exist an interaction between the  $-\text{SO}_3^-$  and amine hydrogens<sup>6</sup> and an increased particle hydrophilicity<sup>7</sup> in the SDP/DAN copolymer

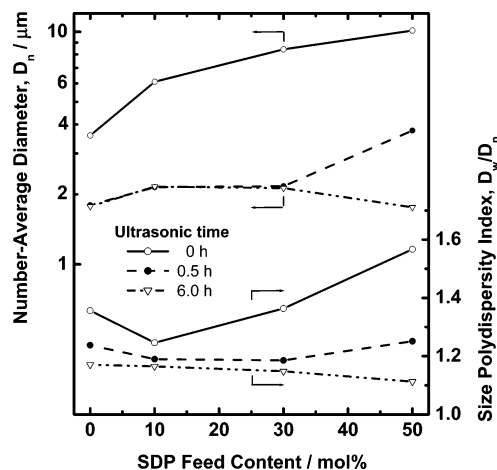


Figure 2. Variation of the number-average diameter ( $D_n$ ) and size polydispersity index ( $D_w/D_n$ ) of SDP/DAN copolymer particles in water with SDP feed content for three ultrasonic dispersion times of 0, 0.5, and 6 h.

particles. Additional free amine groups in DAN units may cause both interactions to be dominant. These result in larger size and looser structure of the microparticles. To prove this hypothesis, the as-prepared particles undergo an ultrasonic dispersion for 0.5 and 6 h. The particle sizes all significantly decrease after the ultrasonic dispersion for 0.5 h, although SDP/DAN (50/50) copolymer particles are still the largest (Figure 2). Upon further prolonging the ultrasonic treatment time to 6 h, the SDP/DAN (50/50) copolymer particles containing the most bulky sulfophenylene side groups show the smallest  $D_n$  of  $1.760 \mu\text{m}$  and smallest  $D_w/D_n$  of 1.1126. Apparently, the size and the distribution of the SDP/DAN (50/50) copolymer particles demonstrate the sharpest decline after the ultrasonic treatment. Under this circumstance, the static repulsion of the sulfonic groups becomes dominant because more sulfonic groups may migrate from inside the loose particles to outside them after the ultrasonic dispersion of 6 h.

The nitrogen adsorption/desorption isotherms (Figure S4, Supporting Information) were used to evaluate the porous structure of the dry microparticles. It seems that SDP/DAN (0/100 and 30/70) polymer microparticles show a typical IVa type isotherm. The broad pore size distribution, calculated from the adsorption branch based on the BJH model, indicates that both polymers do not have uniform pore

structures. It is found from Table S2 (Supporting Information) that the dry PDAN particles have larger BET specific surface area, BJH pore size, and volume than the dry SDP/DAN (30/70) copolymer particles, which coincided with the smaller size of the former in water (Figure 2).

**Properties of Copolymer Microparticles.** The insolubility of the microparticles is strongly influenced by the SDP/DAN ratio (Table S1, Supporting Information). The insolubility becomes higher consistently in DMSO, DMF,  $\text{CHCl}_3$ , and THF with increasing SDP content, even though the SDP homopolymer is completely soluble in  $\text{NH}_4\text{OH}$  and  $\text{H}_2\text{O}$ . These should be ascribed to the introduction of hydrophilic sulfophenylene side group into the polymer chains. Note that the maximal insolubility was observed for the copolymer particles with 40–50 mol % SDP units in  $\text{H}_2\text{SO}_4$  and NMP.<sup>19</sup> That is to say, SDP/DAN (40/60 and 50/50) copolymers are almost insoluble in both solvents, whereas SDP and DAN homopolymers are partially insoluble in the same solvents. Such a unique variation of insolubility suggests the obtainment of real copolymers rather than a simple mixture of both homopolymers. Note that very low solubility or complete insolubility of SDP/DAN copolymers containing 30–50 mol % SDP units in  $\text{CHCl}_3$ , THF,  $\text{NH}_4\text{OH}$ , and  $\text{H}_2\text{O}$  signify their good chemical resistance to nonpolar organic solvents,  $\text{NH}_4\text{OH}$ , and  $\text{H}_2\text{O}$ , which could be very beneficial to  $\text{Ag}^+$  adsorption in the wastewater containing nonpolar organic solvent and alkali.

The bulk electroconductivity of the virgin microparticles of SDP/DAN copolymers increases monotonically from  $3.6 \times 10^{-11}$  to  $3.4 \times 10^{-8} \text{ S cm}^{-1}$  with an increase in SDP concentration from 0 to 50 mol %. This steadily increasing conductivity of the SDP/DAN copolymers in comparison with PDAN should arise from an enhancement of internal doping level from the sulfonic groups<sup>22</sup> and an interaction between the sulfonic groups and cationic radical nitrogen or amine hydrogens on the adjacent polymer chains.<sup>6</sup> However, HCl-doped copolymers exhibit quite different variation of the conductivity with SDP content. As shown in Figure 1, the conductivity of the doped copolymers decreases first and then increases as SDP content rises from 0 to 100%.<sup>19</sup> SDP/DAN (40/60) copolymer has the minimal conductivity of  $3.8 \times 10^{-8} \text{ S cm}^{-1}$ , possibly due to its lowest symmetry of the polymer backbone and shortest conjugation length. This nonmonotonic variation of conductivity with SDP content once again implies that the polymers formed are real copolymers rather than a simple blend of both homopolymers. Noteworthily, all of the HCl externally doped microparticles exhibit much higher conductivity than sulfonic group internally doped microparticles, suggesting an imperfect internal doping from sulfonic groups with lower mobility and concentration than HCl.

The thermogravimetry of SDP/DAN (0/100 and 30/70) polymer microparticles in air has been evaluated. Compared with PDAN, which has only one weight loss at around 500 °C, the SDP/DAN (30/70) copolymer has an additional small weight loss at around 300 °C, which is caused by the elimination of the phenylenesulfonic side groups.<sup>18,19,23</sup> It is

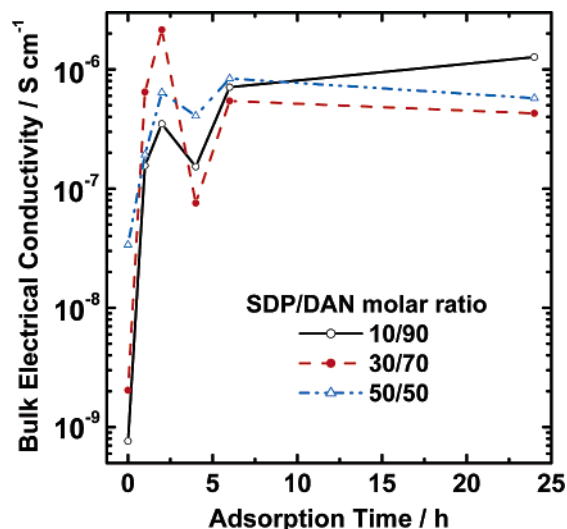


**Figure 3.** Bulk electrical conductivity of as-polymerized SDP/DAN copolymer particles adsorbing silver for different adsorption times in 25 mL of  $\text{AgNO}_3$  solution at pH 5.3 and an initial  $\text{Ag}^+$  concentration of 84 mM at 30 °C.

found that the decomposition temperature ( $T_d$ ) and peak temperature ( $T_m$ ), due to the breakage of polymer backbone, and char yield all rise with incorporating SDP units (Table S2, Supporting Information), whereas the corresponding maximum decomposition rate decreases, which is opposite to the variation of thermostability of SDP/AN copolymers with SDP incorporation.<sup>19</sup> This implies that the interaction between the phenylenesulfonic acid and amino/imino groups, which are very useful for  $\text{Ag}^+$  reactive adsorption, becomes stronger with adding SDP units. It is also noticed that the polymers do not exhibit any weight loss until 250 °C in air, demonstrating a good thermostability, which is favorable for their application in a high-temperature environment.

**Silver Ion Reactive Adsorption of Copolymer Microparticles.** The strong  $\text{Ag}^+$  adsorbability on the SDP/DAN polymer particles has been confirmed by a great change of their crystalline structure,<sup>24</sup> conductivity<sup>11</sup> and char yield at elevated temperature. The particles reactively adsorbing silver ion display much higher crystallinity, conductivity, and char yield at 700 °C (Figure 3, and Table S2 and Figure S3 of the Supporting Information). The X-ray diffractograms of the particles adsorbing  $\text{Ag}^+$  exhibit almost no peaks at 13.0° and 23.9° but three additional, much stronger peaks at 38°, 44°, and 64°, respectively, corresponding to (111), (200), and (220) lattice planes of Ag crystals, proving the reduction of  $\text{Ag}^+$  by the free amino ( $-\text{NH}_2$ ) groups on the particles.<sup>24</sup>

It is seen from Figure 3 that the conductivity of the copolymer microparticles increases dramatically during the initial  $\text{Ag}^+$  adsorption of 2 h and then stays almost constant after passing through a minimum adsorption at 4 h. The complicated variation of conductivity can be explained by the growing and doping mechanism of reduced Ag crystal. The mechanism involves two stages: (1) the reduction of  $\text{Ag}^+$  on the free amino groups, accompanying with the formation of Ag crystal nucleus, and (2) the growth of Ag around the crystal nucleus. During an early period of

(22) Yue, J.; Epstein, A. J. *J. Am. Chem. Soc.* **1990**, *112*, 2800.

(23) Chen, S. A.; Hwang, G. H. *Macromolecules* **1996**, *29*, 3950.

(24) Li, X. G.; Huang, M. R.; Li, S. X. *Acta Mater.* **2004**, *52*, 5363.

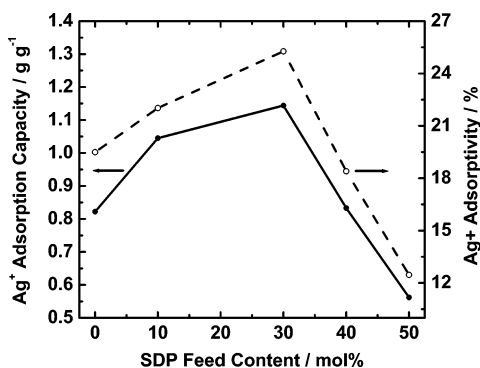


**Figure 4.** The change of  $\text{Ag}^+$  adsorption capacity and adsorptivity on SDP/DAN polymer particles not undergoing ultrasonic treatment with SDP content in 25 mL of  $\text{AgNO}_3$  solution at pH 5.3 and an initial  $\text{Ag}^+$  concentration of 84 mM at 30 °C for 24 h.

adsorption, the unique distribution of fine Ag crystal as a conducting channel results in the drastic improvement of conductivity. With the growth of Ag crystal, the atactic crystal aggregate causes the partial decline in conductivity. After a certain adsorption time, the further increasing Ag content in the particles has little effect on conductivity. In addition, it is interesting that the conductivity of the Ag-adsorbing particles is nearly the same as that of HCl-doped particles (Figure 1). Consequently, the reactive adsorption of  $\text{Ag}^+$  on the polymer particles may be regarded as a new doping method for the preparation of conducting materials.<sup>2,11</sup>

$\text{Ag}^+$ -adsorbing SDP/DAN (30/70) copolymer particles demonstrate much lower decomposition temperatures but much higher decomposition rate and char yield at 700 °C (Table S2, Supporting Information), validating the existence of Ag and  $\text{Ag}^+\text{NO}_3^-$  in the particles, because the  $\text{Ag}^+\text{NO}_3^-$  would lower the stability of the particles while the Ag and  $\text{Ag}^+$  will significantly enhance the residual weight percentage. In summary, these results strongly indicate a true Ag uptake onto the microparticles. In particular, the  $\text{Ag}^+$  adsorption on the microparticles could be significantly optimized by regulating SDP/DAN ratio, adsorption time, particle size, and pH, as elaborated below.

**Optimization of the SDP/DAN Comonomer Ratio.** As shown in Figure 4, the  $\text{Ag}^+$  adsorption capacity and adsorptivity on the microparticles increase first and then decrease with increasing SDP content. Particularly, the SDP/DAN (30/70) copolymer particles possess the maximal adsorption capacity and adsorptivity up to 1.144  $\text{g g}^{-1}$  and 25.3% respectively, an enhancement of 30–40% compared with PDAN. The enhancement of adsorbability may be attributed to the optimal combination of free amino and sulfonic groups on the copolymer chains (Table 1), which is beneficial to the efficient interaction of  $\text{Ag}^+$  and free amino/sulfonic groups. Therefore, the introduction of sulfophenylene side group into the PDAN backbone can effectively enhance the reactivity of the microparticles with  $\text{Ag}^+$ . With further increasing SDP content from 30 to 50 mol %, the amount of the amino/imino ( $-\text{NH}_2/-\text{NH}-$ ) groups must become less, resulting in a decreased  $\text{Ag}^+$  adsorbability. The nonmonotonic variation of the  $\text{Ag}^+$  adsorbability with SDP content may indicate that the SDP/DAN polymers are genuine copolymers.

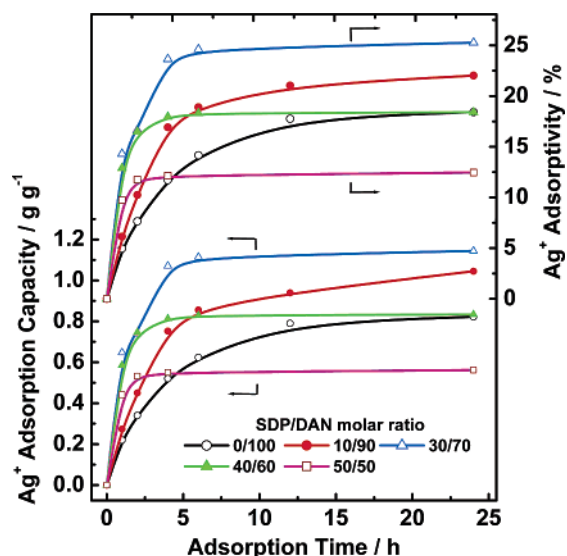


**Figure 5.** Time-dependent adsorption of SDP/DAN polymer particles of 50 mg in 25 mL of  $\text{AgNO}_3$  solution at pH 5.3 and an initial  $\text{Ag}^+$  concentration of 84 mM at 30 °C.

**Table 2.** Lagergren Model Equations of  $\text{Ag}^+$  Adsorption Kinetics on the SDP/DAN Copolymer Particles

SDP/DAN feed molar ratio	Lagergren equation	adsorption rate constant/ $\text{h}^{-1}$	correlation coefficient	SD
0/100	$Q_t = 832(1 - e^{-0.187t})$	0.187	0.987	0.278
10/90	$Q_t = 1045(1 - e^{-0.179t})$	0.179	0.955	0.280
30/70	$Q_t = 1144(1 - e^{-0.603t})$	0.603	0.987	0.271
40/60	$Q_t = 834(1 - e^{-0.765t})$	0.765	0.997	0.153
50/50	$Q_t = 562(1 - e^{-0.732t})$	0.732	0.952	0.507

A similar effect can also be observed in Figure 5 for the function of the  $\text{Ag}^+$  adsorption capacity and adsorptivity against adsorption time. SDP/DAN (30/70) copolymer microparticles indeed exhibit the maximal  $\text{Ag}^+$  adsorbability in the whole adsorption time. Under the same adsorption condition, the PDAN takes 12 h to reach adsorption equilibrium while SDP/DAN (30/70 and 50/50) copolymers take 6 and 2 h, respectively. The high adsorption rate of the copolymers should originate from the introduction of bulky sulfophenylene groups into the polymer structure, which accelerates the diffusion of  $\text{Ag}^+$  inside the particles. Besides, the faster adsorption equilibrium of the copolymers with SDP content of 30–50 mol % may be attributable to fewer amino/imino groups. Table 2 lists the  $\text{Ag}^+$  adsorption kinetic parameters of the microparticles, and it can be discovered that the microparticles with SDP feed content of 40–50 mol % exhibit the highest adsorption rate of  $\text{Ag}^+$ . The  $\text{Ag}^+$  adsorption on the SDP/DAN (40/60) copolymer microparticles fits the Lagergren model best based on correlation coefficient and standard deviation in comparison with PDAN– $\text{Ag}^+$  adsorption.

Moreover, SDP/DAN (30/70) copolymer microparticles exhibit different adsorption behavior in an initial  $\text{Ag}^+$  concentration range of 0–100 mM compared to PDAN. As shown in Figure 6, the PDAN microparticles adsorb  $\text{Ag}^+$  more efficiently than the SDP/DAN (30/70) copolymer microparticles at an initial  $\text{Ag}^+$  concentration of lower than 52 mM, whereas the copolymer microparticles adsorb  $\text{Ag}^+$  more efficiently at an initial  $\text{Ag}^+$  concentration of higher than 52 mM. It is considered that at the low  $\text{Ag}^+$  concentra-



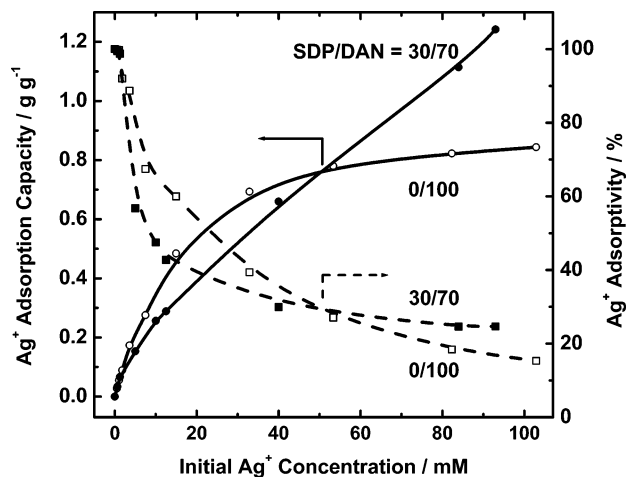


**Figure 6.** Effect of initial  $\text{Ag}^+$  concentration on  $\text{Ag}^+$  adsorption on 50 mg of SDP/DAN (0/100 and 30/70) polymer particles in 25 mL of  $\text{AgNO}_3$  solution at pH 5.3 and 30 °C for an adsorption time of 24 h.

tion, the reactive sites on the particle surface dominate the adsorbability. The larger specific surface area and then higher active site concentration on PDAN particles lead to stronger adsorbability of  $\text{Ag}^+$  than the copolymer particles (Table S2, Supporting Information). At high  $\text{Ag}^+$  concentration, the ion concentration is high enough for  $\text{Ag}^+$  to easily diffuse into the inside of the particles, especially of the loose SDP/DAN (30/70) copolymer particles in water (Figure 2). This results in higher adsorbability of the copolymer particles than PDAN microparticles. Therefore, the  $\text{Ag}^+$  adsorption is determined by several key factors such as  $\text{Ag}^+$  concentration as well as the molecular structure, specific surface area, and compactness of the particles.<sup>25</sup> Moreover, Langmuir and Freundlich equations are used to establish the relationship between ion concentration and adsorption process (Table S3, Supporting Information). It appears that PDAN- $\text{Ag}^+$  fits the Langmuir model better while SDP/DAN (30/70)- $\text{Ag}^+$  fits the Freundlich model better.

The SDP/DAN (30/70) copolymer microparticles exhibit smaller specific surface area and pore volume (Table S2, Supporting Information) but higher  $\text{Ag}^+$  adsorbability than PDAN microparticles, indicating that the  $\text{Ag}^+$  adsorption on the microparticles should be reactively controlled. In fact, it is reported that the carbon fiber also exhibits a similar variation of  $\text{Ag}^+$  adsorbability with its surface area.<sup>9</sup> The  $\text{Ag}^+$  adsorbability ( $1360 \text{ mg g}^{-1}$ ) on highly activated carbon fiber with a surface area of  $115 \text{ m}^2 \text{ g}^{-1}$  is much stronger than that ( $403 \text{ mg g}^{-1}$ ) on the fiber with a much larger surface area of  $1284 \text{ m}^2 \text{ g}^{-1}$ .

**Effect of Particle Size.** As discussed above, ultrasonic treatment can effectively disperse larger particles into smaller and more narrowly distributed particles (Figure 4) and therefore greatly increase the specific surface area. The effect of particle size on  $\text{Ag}^+$  adsorption on the polymer particles is illustrated in Figure 7. It is found that both the adsorption capacity and adsorptivity of SDP/DAN (10/90) copolymer microparticles demonstrate the most remarkable increase of 18% after ultrasonic dispersion for 6 h. In fact, the SDP/DAN (10/90) copolymer particles exhibit the strongest  $\text{Ag}^+$

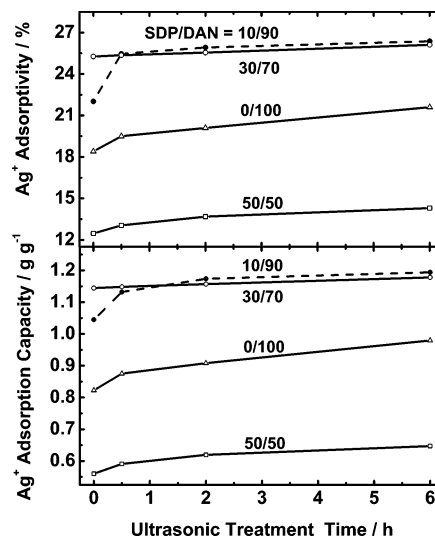


**Figure 7.** Effect of particle size on  $\text{Ag}^+$  adsorption onto the SDP/DAN polymer microparticles following an ultrasonic treatment in 25 mL of  $\text{AgNO}_3$  solution at pH 5.3 and an initial  $\text{Ag}^+$  concentration of 84 mM at 30 °C for 24 h.

**Table 3.** Effect of pH Value on  $\text{Ag}^+$  Adsorption on 50 mg of SDP/DAN Polymer Microparticles in 25 mL of  $\text{AgNO}_3$  Solution at an Initial  $\text{Ag}^+$  Concentration of 84 mM at 30 °C for 24 h

pH	ultrasonic treatment time/h	adsorbability	values for SDP/DAN feed molar ratios			
			0/100	10/90	30/70	50/50
5.3	0	$Q/\text{mg g}^{-1}$	823	1045	1144	562
		$q/\%$	19.5	23.4	25.3	12.5
6.3	0	$Q/\text{mg g}^{-1}$	1635	1322	1355	614
		$q/\%$	37.2	29.2	29.9	13.6
7.0	0	$Q/\text{mg g}^{-1}$	1670	1339	1428	998
		$q/\%$	38.0	29.5	31.5	22.0
7.0	0.5	$Q/\text{mg g}^{-1}$	1684	1348	1446	1048
		$q/\%$	38.2	29.8	31.9	23.2

adsorbability during ultrasonic dispersion of 2–6 h. Less enhancement of  $\text{Ag}^+$  adsorbability on the copolymers with SDP content of 30–50 mol % after the ultrasonic dispersion could be associated with their fewer amino/imino groups that could effectively react with  $\text{Ag}^+$ . The largest increase in  $\text{Ag}^+$  adsorbability of SDP/DAN (10/90) copolymer particles for the adsorption time of 24 h is further verified by ultrasonic dispersion for 0.5 h (Figure S5, Supporting Information). It also demonstrates that all of the smaller polymer particles formed after ultrasonic dispersion for 0.5 h exhibit a faster adsorption rate and stronger adsorbability of  $\text{Ag}^+$  than as-prepared particles. A shorter time was required to reach adsorption equilibrium on the smaller ultrasonic particles. In conclusion, the particle size has the strongest effect on  $\text{Ag}^+$  adsorption on SDP/DAN polymer particles.

**Effect of  $\text{Ag}^+$  Solution pH.** The effect of pH on  $\text{Ag}^+$  adsorption on the microparticles is illustrated in Table 3. It reveals a significant increase in the  $\text{Ag}^+$  adsorbability with increasing pH. From pH 5.3 to 6.3, the microparticles containing more DAN units show greater enhancement of the  $\text{Ag}^+$  adsorbability than those containing more SDP units, while from pH 6.3 to 7.0, the adsorbability enhancement of the microparticles containing more SDP units becomes larger. This indicates that the mechanism of adsorption in different pH media is different. As shown in Figure 8, besides the complex and redox functions between  $\text{Ag}^+$  and amino/imino groups,  $\text{Ag}^+$  could replace some  $\text{Na}^+$  or  $\text{H}^+$  in sulfophenylene

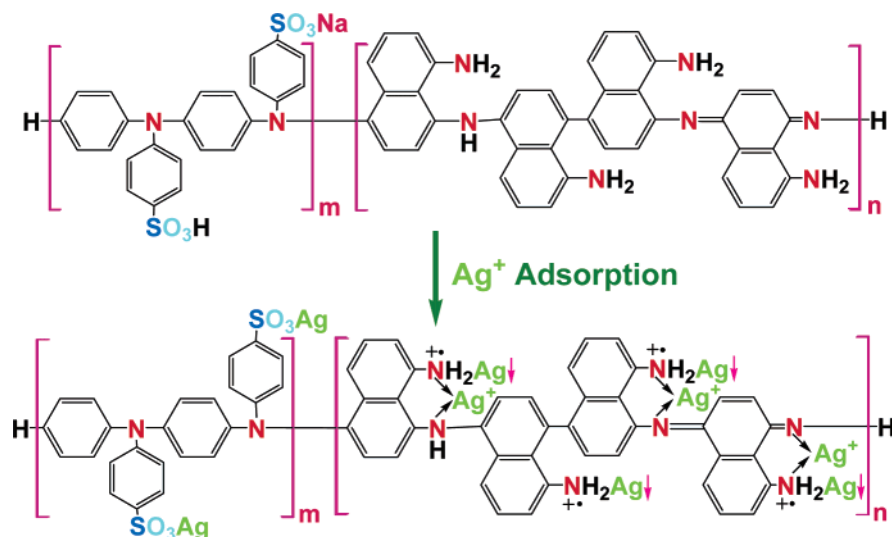


**Figure 8.** Redox, complexation, and exchange reactive adsorptions of silver ions on nominal SDP/DAN copolymers prepared by a chemically oxidative polymerization.

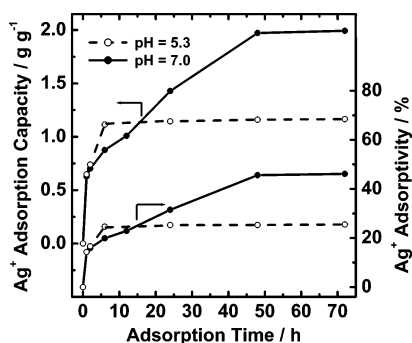


**Figure 9.** Time-dependent adsorption of 50 mg of SDP/DAN (30/70) copolymer particles in 25 mL of  $\text{AgNO}_3$  solution at two pH values and an initial  $\text{Ag}^+$  concentration of 84 mM, i.e., the initial  $\text{Ag}^+$  of 42 mmol  $\text{g}^{-1}$  of the microparticles at 30 °C.

side groups. Generally, the low pH is disadvantageous to the replacement function owing to strong protonation of free amino groups on the copolymers. With raising the pH from 5.3 to 6.3, the weakened protonation of free amino groups greatly improves the  $\text{Ag}^+$  adsorption. Upon further raising the pH to 7.0, the replacement function becomes dominated in the  $\text{Ag}^+$  adsorption. However, ultrasonic dispersion at pH 7 only slightly improves the adsorbability.

As observed in Figure 9, the SDP/DAN (30/70) copolymer particles can realize adsorption equilibrium in 6 and 48 h at pH 5.3 and 7.0, respectively. Although the adsorption rate is slightly slower at 7.0 than at 5.3, the equilibrium adsorbability at 7.0 is much higher. Perhaps the diffusion of  $\text{Ag}^+$  into the particles is more strongly affected in higher pH solution, resulting in slower adsorption at pH 7.0. In particular, after adsorption for 48 h at pH 7.0, the  $\text{Ag}^+$  adsorption capacity reaches 2.0  $\text{g g}^{-1}$ , significantly exceeding the highest  $\text{Ag}^+$  adsorbance (1.36  $\text{g g}^{-1}$ ) onto the activated carbon fiber<sup>9</sup> at the initial  $\text{Ag}^+$  of 100 mmol  $\text{g}^{-1}$  of the fiber for a long adsorption time of 30 days. It can be inferred that the copolymer microparticles should exhibit even stronger  $\text{Ag}^+$  adsorbability if at the same adsorption conditions as the carbon fiber. The SDP/DAN (30/70) copolymer particles with much smaller specific surface area exhibit stronger  $\text{Ag}^+$  adsorbability than activated carbon fiber with much larger specific surface area (115  $\text{m}^2 \text{g}^{-1}$ ), signifying that the  $\text{Ag}^+$  adsorption mechanism

on the particles is different from that on the carbon fiber. Novel reactive interaction between  $\text{Ag}^+$  and  $-\text{NH}_2/-\text{NH}-/-\text{SO}_3\text{H}$  groups on the particles should be predominant.

### Conclusions

A series of high-performance copolymer microparticles from SDP and DAN monomers has been synthesized successfully by a facile chemical oxidation precipitation polymerization with  $(\text{NH}_4)_2\text{S}_2\text{O}_8$  as an oxidant. DAN monomer exhibits stronger polymerizability than SDP monomer during their oxidative copolymerization, leading to higher DAN content in the copolymer than feed content. The polymerization yield, insolubility, electroconductivity, and thermostability of the copolymer microparticles significantly depend on the comonomer ratio. A systematically nonmonotonic variation of the polymerization solution potential, IR spectrum, particle size, insolubility, conductivity, and  $\text{Ag}^+$  adsorbability of the polymers with the SDP/DAN ratio suggests that the polymers obtained are real copolymers rather than simple mixtures of both homopolymers. The copolymer particles display good chemical and heat resistances. The presence of bulky sulfophenylene side groups in the copolymers allows there to be a loose particle structure, which contributes to the effective diffusion of  $\text{Ag}^+$  into the particles and therefore enhances the adsorption capacity and rate at high  $\text{Ag}^+$  concentration. Reductions of the particle size and  $\text{Ag}^+$  solution acidity both strengthen the interaction between  $\text{Ag}^+$  and microparticles and accordingly achieve further stronger  $\text{Ag}^+$  adsorbability. The amount of  $\text{Ag}^+$  adsorbed by SDP/DAN (30/70) copolymer particles can reach 2.0  $\text{g g}^{-1}$ , which is the highest silver adsorption capacity seen thus far. Particularly, the SDP/DAN copolymers with abundant amino, imino, and sulfonic groups possess extremely powerful  $\text{Ag}^+$  reactive adsorbability, which is attributed to an optimal combination of (1) complexation between  $\text{Ag}^+$  ion and amino or imino groups, (2) the redox reaction between  $\text{Ag}^+$  and free  $-\text{NH}_2$  group, and (3) replacement of  $\text{Na}^+$  or  $\text{H}^+$  on sulfonic groups by  $\text{Ag}^+$ . The SDP/DAN copolymer microparticles have presented a great application potential in removal and recycle of noble or heavy metallic ions from wastewater. Furthermore, it can be



predicted that the microparticles could served as a novel support for enzyme immobilization, due to their large surface-to-volume ratio and large amounts of amino/imino/sulfonic groups on the particles that give a very simple, mild, and time-saving immobilization of enzyme.<sup>26</sup>

**Acknowledgment.** The project was supported by the National Natural Science Foundation of China (20274030). X.G.L. thanks Prof. Dr. Roy G. Gordon, Harvard University, for his valuable help.

---

(26) Oh, J.-T.; Kim, J.-H. *Enzyme Microbial Technol.* **2000**, *27*, 356.

**Supporting Information Available:** Insolubility and solution color of SDP/DAN copolymer microparticles, isotherm model equations for Ag<sup>+</sup> adsorption on the microparticles in water, the thermostability of the dry microparticles, FT-IR spectra of the microparticles, UV-vis absorption spectra of the copolymers in NMP, WAXD patterns of the dry microparticles before and after the adsorption of silver ions, nitrogen adsorption-desorption isotherm and pore structure of the dry microparticles, and time dependent adsorption of a series of the microparticles before and after ultrasonic treatment. This material is available free of charge via the Internet at <http://pubs.acs.org>.

CM050813S